SKI Report 2006:30

Research

Benchmarking - a validation of UTDefect

Jonas Niklasson
Anders Boström
Håkan Wirdelius

June 2006

ISSN 1104-1374
ISRN SKI-R-06/30-SE

SKI

SKI perspective

Background

Mathematical modelling is an important tool for developing NDT systems and in the end to get more reliable testing systems. It is also important in the situation of inspection qualification to get more flexibility and effectiveness.

SKI has for many years been supporting research for development of a model for ultrasonic testing. SKI sees the importance and the benefits in modelling testing situations and bechmarking projects are an important tool for verification.

Purpose of the project

The purpose of the project is to verify the UTDefect ultrasonic model towards experimental data through a benchmark study.

Results

The results show good correlation to experimental data in most of the cases. It also gives us information on some cases where continuous development is necessary.

Project information

Responsible for the project at SKI has been Peter Merck.
SKI reference: 14.43 - 200443103

SKI Report 2006:30

Research

Benchmarking - a validation of UTDefect

Jonas Niklasson[1]
Anders Boström[2]
Håkan Wirdelius[3]

1
Enmesh AB
Bror Nilssons Gata 5
SE-41755 Göteborg

2
CHALMERS UNIVERSITY OF TECHNOLOGY
Department of Applied Mechanics
SE-412 96 Göteborg

3
CHALMERS UNIVERSITY OF TECHNOLOGY
Department of Materials and Manufacturing Technology
SE-412 96 Göteborg

June 2006

Table of content

Summary

New and stronger demands on reliability of used NDE/NDT procedures and methods have stimulated the development of simulation tools of NDT. Modelling of ultrasonic non-destructive testing is useful for a number of reasons, e.g. physical understanding, parametric studies and in the qualification of procedures and personnel. The traditional way of qualifying a procedure is to generate a technical justification by employing experimental verification of the chosen technique. The manufacturing of test pieces is often very expensive and time consuming. It also tends to introduce a number of possible misalignments between the actual NDT situation and the proposed experimental simulation.

The UTDefect computer code (SUNDT/simSUNDT) has been developed, together with the Dept. of Mechanics at Chalmers University of Technology, during a decade and simulates the entire ultrasonic testing situation. A thorough validated model has the ability to be an alternative and a complement to the experimental work in order to reduce the extensive cost. The validation can be accomplished by comparisons with other models, but ultimately by comparisons with experiments. This project addresses the last alternative but provides an opportunity to, in a later stage, compare with other software when all data are made public and available.

The comparison has been with experimental data from an international benchmark study initiated by the World Federation of NDE Centers. The experiments have been conducted with planar and spherically focused immersion transducers. The defects considered are side-drilled holes, flat-bottomed holes, and a spherical cavity. The data from the experiments are a reference signal used for calibration (the signal from the front surface of the test block at normal incidence) and the raw output from the scattering experiment. In all, more than forty cases have been compared.

The agreement between UTDefect and the experiments was in general good (deviation less than 2dB) when the incident angle of the pressure wave in the fluid were kept low, i.e. to generate longitudinal (P) waves into the object. When the angle was increased, in order to generate shear (S) waves into the test blocks, the discrepancy increased up to 4dB. This tendency were found both for planar and focused transducers acting on test blocks with either side-drilled holes (SDH) or flat-bottomed holes and was also reported by the other modelers. In the case of the spherical cavity, the differences between the experimental data and UTDefect in the two cases are 5.0 dB and 3.6 dB, respectively. These large discrepancies are more difficult to explain by means of modeling error or experimental errors and the matter needs further investigation.

Sammanfattning

Nya och starkare krav på tillförlitligheten hos de system för oförstörande provning och procedurer som tillämpas vid den återkommande provningen i kärnkraftsindustrin har stimulerat utvecklandet av olika simuleringshjälpmedel. Matematisk modellering av oförstörande provning har under de senaste åren uppmärksammats som ett kostnadseffektivt och kraftfullt verktyg inom ett antal tillämpningsområden. Matematisk modellering är en förutsättning för mer omfattande parameterstudier, kan ge ökad förståelse för det fysikaliska förloppet och tillämpas i kvalificeringsprocessen. Förutom att det konventionella tillvägagångssättet vid kvalificeringar innefattar tillverkning av dyra testblock tenderar dessa dessutom att introducera signalsvar som inte är tillräckligt realistiska eller till och med direkt felaktiga, beroende på att ett antal parametrar hos de artificiella defekterna är svåra att styra på ett tillförlitligt sätt vid tillverkningen.

Programvaran UTDefect (SUNDT/simSUNDT) har under de senaste två årtionden utvecklats i samarbete med Institutionen Tillämpad Mekanik vid Chalmers. Denna programvara möjliggör simulering av hela provningssituationen som utförs med ultraljudsteknik. Förutsättningen för att man fullt ut skall kunna tillämpa matematisk modellering i kvalificeringsarbetet är att programvaran är validerad i någon form. Detta kan ske i jämförelse med annan programvara baserad på andra idealiseringar eller antaganden eller i direkt jämförelse med experimentella data. Problemet som man ställs inför är att tillgängligt antal verkliga sprickor är mycket begränsat och simulerade data jämförs tendensiöst mot experimentella data från artificiella sprickor.

”World Federation of NDE Centers” har startat ett omfattande valideringsprojekt som är öppet för alla att delta i. Detta projekt möjliggör en jämförande studie med olika programvaror som simulerar en realistisk OFP situation och motsvarande experimentellt framtagna mätdata. Man har valt att inledningsvis använda sig av mycket enkla och väldefinierade defekter (sidoborrat hål, flatbottnade hål och sfärisk kavitet) tillsammans med ett väldefinierat randvillkor på ytan som fås genom att välja just immersions-provning (både plan och fokuserad immersionssökare). På detta vis undviker man att validera den kompletta modellen av signalsvar eftersom denna är komplex och beroende av ett antal enskilda komponenter (sändare, mottagare, kontaktvillkor, modell av defekt o.s.v.). Deltagandet i detta projekt möjliggör således validering av själva modelleringen av reflektorn som utgörs av en väldefinierad geometrisk kropp.

Utfallet av denna jämförande studie ger att UTDefect generellt gav god överensstämmelse med de experimentella värdena (avvikelse mindre än 2 dB) under förutsättning att sökaren inte positionerades i syfte att generera transversalvågsljud i soliden (S). Detta sammanföll med ett infall mot ytan som översteg 13° (aluminium och 30° transversalvågsljud) då avvikelser på 4 dB kunde identifieras. Ovan gäller för SBH oavsett om sökaren var fokuserad eller ej. För det flatbottnade hålen (FBH) var avvikelsen mindre än 1.5 dB. Detta troligen beroende på att sökarna (både plan och fokuserad immersionssökare) enbart positionerades för att generera ovinklat longitudinalvågsljud (P). För de två experimentella jämförelserna med sfärisk kavitet är avvikelserna förvånansvärt stora (5 respektive 3.6 dB). Dessa diskrepanser går inte att ge en enkel förklaring till och bör studeras närmare.

Den troligaste förklaringen till skillnaderna ovan är den höga känsligheten för avvikelser från exakta värden på vinklar. Eftersom samma tendens kunde identifieras även för de andra programvarorna kan förklaringen ligga i svårigheter att experimentellt generera ljud med hög noggrannhet med avseende på den infallande vinkeln. En annan är den att vinkeln som är givna för mätdata tagits fram rent experimentellt medan vinklarna som använts vid simuleringarna baserar sig på Snells lag för centrumstrålen av ljudet.

Introduction

Modelling of ultrasonic non-destructive testing is useful for a number of reasons, e.g. physical understanding, parametric studies, and the qualification of procedures and personnel. During the last two decades a number of models have therefore emerged internationally, at least in the United Kingdom, Germany, France, USA, and Sweden. An important issue regarding all models is the validation, i.e. securing that the results of the model and the corresponding computer programs are correct. This can be accomplished by comparisons with other models, but ultimately by comparisons with experiments. Some limited efforts were undertaken more than ten years ago to compare and evaluate some models and corresponding computer programs within the PISC 3 project, see Lakestani (1992).

More recently, benchmarking projects have been initiated by the World Federation of NDE Centers (http://www.wfndec.org), and some of these efforts have been reported at the last three conferences in the yearly series Review of Progress in Quantitative Nondestructive Evaluation. Experiments have been conducted on some simple defects, side-drilled holes, flat-bottomed holes, and spheres, in simple immersion testing with unfocussed and focussed probes. These results are made public so that models can be compared with the experiments. About six models have contributed with results at the past few conferences (see the references when the results are discussed in the following).

The computer program UTDefect has been developed during more than a decade, see a number of SKI reports (1995, 1997, 2000, 2001). It uses some integral and integral equation methods to model the scattering by a number of simply shaped defects: strip-like, rectangular, and circular cracks, spheres, spheroids, and side-drilled holes. Also strip-like and rectangular cracks in an anisotropic component are included. The probes may be contact or immersion of any type and angle. The output is conventional A, B, and C scans. Both time and frequency domain output can be obtained. The methods employed are essentially exact within the assumptions of linear elasticity, piston probe models, idealised defects, etc. In contrast, the other models reported at the conferences mentioned above mostly use some approximations, like the Kirchhoff approximation for defect scattering and various probe field approximations.

UTDefect has been compared with experiments and other models in a few cases, see the reports, but not very systematically or extensively. Thus it seems appropriate to pursue this in more detail now when the opportunity has arisen with the WFNDEC experiments. This is thus the aim of the present report.

In the WFNDEC experiments both planar and focussed probes are used in an immersion setting and the results are calibrated with the front echo signal from the test block at normal incidence. Focussed immersion probes and the front echo calibration are not included in UTDefect so part of the present project is to make these extensions of UTDefect.

Probe modeling

The transducers used in the benchmark study are of immersion type and both planar and focused transducers are considered. In addition, the damping of the fluid is taken into account. In UTDefect, only planar immersion transducers without fluid damping are implemented so the damping and focusing effects must be modeled. Assume that the speed of sound in the fluid is c_F, the density is ρ_F, and that the damping parameter is α. In addition, time-harmonic conditions are assumed and the factor $e^{-i\omega t}$ is omitted throughout.

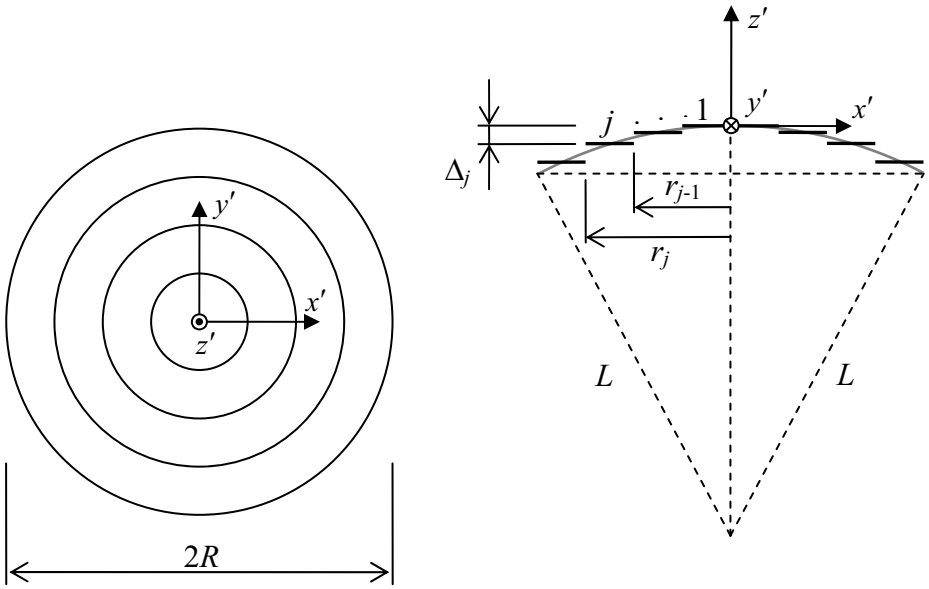

Figure 1: Division of the spherically focused transducer.

The focused probes used in the benchmark study are spherically focused. As a model of the probe, the spherical surface is divided into N coplanar rings (see Figure 1 where the case $N = 4$ is shown). The radius of the transducer is R and the geometrical focal length is L. The radius r_j and the distance between ring j and ring 1 Δ_j along the focal axis are given by

$$\begin{aligned} r_j &= R\frac{j}{N}, && j = 1,\ldots,N, \\ \Delta_1 &= 0, \\ \Delta_j &= L - \sqrt{L^2 - (r_{j-1} + r_j)^2 / 4}, && j = 2,\ldots,N. \end{aligned} \tag{1}$$

Assuming a constant pressure P_0 on each ring, the pressure distribution in the fluid from disk j is given by (assuming no damping)

$$P_j(x', y', z') = P_0 \int_{-\infty}^{\infty}\int_{-\infty}^{\infty} \frac{\xi'_{0j}(s(q', p'))}{4\pi k h'(s(q', p'))} e^{i(q'x' + p'y' - h'(s(q', p'))z')}\, dq'\, dp', \tag{2}$$

where

$$
\begin{aligned}
&\xi'_{01}(s) = 2kh'(s) r_1^2 \frac{\mathrm{J}_1(C_1(s))}{C_1(s)}, \\
&\xi'_{0j}(s) = 2kh'(s) \left(r_j^2 \frac{\mathrm{J}_j(C_j(s))}{C_j(s)} - r_{j-1}^2 \frac{\mathrm{J}_{j-1}(C_{j-1}(s))}{C_{j-1}(s)} \right) \mathrm{e}^{-\mathrm{i}h'(s)\Delta_j}, \quad j = 2, \ldots, N, \\
&k = \frac{\omega}{c_\mathrm{F}}, \\
&s(q', p') = \sqrt{(q')^2 + (p')^2}, \\
&C_j(s) = r_j\, s, \qquad\qquad j = 1, \ldots, N, \\
&h'(s) = \sqrt{k^2 - s^2}, \qquad\qquad \operatorname{Im} h' \geq 0.
\end{aligned}
\tag{3}
$$

Above, $\mathrm{J}_j(x)$ is the cylindrical Bessel function of the first kind and order j. The sound field radiated by the focused transducer is obtained by summing the contributions from all the rings. The result is

$$
\begin{aligned}
&P(x', y', z') = \sum_{j=1}^{N} P_j(x', y', z') = P_0 \int_{-\infty}^{\infty} \int_{-\infty}^{\infty} \frac{\xi'_0(s(q', p'))}{4\pi k h'(s(q', p'))} \mathrm{e}^{\mathrm{i}(q'x' + p'y' - h'(s(q', p'))z')} \, \mathrm{d}q' \, \mathrm{d}p', \\
&\xi'_0(s) = \sum_{j=1}^{N} \xi'_{0j}(s).
\end{aligned}
\tag{4}
$$

All transducer models in UTDefect prescribe the traction on the surface of the elastic component. As a consequence, the reflection and transmission of the waves from the model above by an elastic half-space must be considered. In order to enable tilt of the transducer, two coordinate systems are introduced (see Figure 2). The $x'y'z'$ system is attached to the transducer as above and the *xyz* system is attached to the surface of the elastic half-space. The $x'y'z'$ system is rotated an angle β around the *y* axis relative the *xyz* system and the distance from the transducer to the half-space is *D*. The speeds of the P and S waves in the half-space are c_p and c_s, respectively, and the density is ρ.

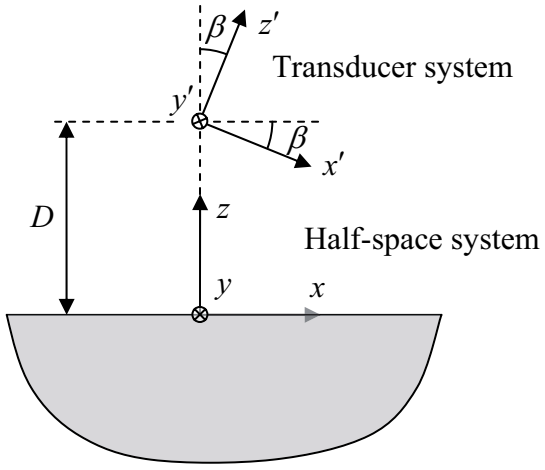

Figure 2: The transducer and half-space.

By enforcing continuity of the displacement and traction in the z direction, and that the traction is zero in the x and y directions, the field in the fluid and the half-space are obtained as

$$
\begin{aligned}
&P(x,y,z) = P^{(\mathrm{i})}(x,y,z) + P^{(\mathrm{r})}(x,y,z) = \\
&\qquad P_0 \int_{-\infty}^{\infty}\int_{-\infty}^{\infty} \frac{\xi_0(q,p)}{4\pi k h}\left(\mathrm{e}^{-\mathrm{i}hz} + T\mathrm{e}^{\mathrm{i}hz}\right)\mathrm{e}^{\mathrm{i}(qx+py)}\,\mathrm{d}q\,\mathrm{d}p, \qquad z \geq 0, \\
&\boldsymbol{u}(x,y,z) = \sum_{j=1}^{3}\int_{-\infty}^{\infty}\int_{-\infty}^{\infty} \frac{\xi_j(q,p)}{k_j h_j}\boldsymbol{\varphi}_j^-(q,p,x,y,z)\,\mathrm{d}q\,\mathrm{d}p, \qquad z \leq 0, \\
&\xi_0(q,p) = \xi_0'(s(q\cos\beta + h\sin\beta, p))\,\mathrm{e}^{\mathrm{i}hD}, \\
&\xi_1(q,p) = 0, \\
&\xi_2(q,p) = -4\mathrm{i}P_0\,\frac{k_\mathrm{s}^2 h_\mathrm{p} h_\mathrm{s} s}{k c_\mathrm{s}^2(\rho_\mathrm{F} h_\mathrm{p} k_\mathrm{s}^4 + \rho h R)}\,\xi_0'(q\cos\beta + h\sin\beta, p), \\
&\xi_3(q,p) = 2\sqrt{\frac{k_\mathrm{p}}{k_\mathrm{s}}}P_0\,\frac{k_\mathrm{s}^2 h_\mathrm{p}(k_\mathrm{s}^2 - 2s^2)}{k c_\mathrm{s}^2(\rho_\mathrm{F} h_\mathrm{p} k_\mathrm{s}^4 + \rho h R)}\,\xi_0'(q\cos\beta + h\sin\beta, p), \qquad (5) \\
&s(q,p) = \sqrt{q^2 + p^2}, \\
&h(s) = \sqrt{k^2 - s^2}, \quad \mathrm{Im}\,h \geq 0, \\
&h_\mathrm{p}(s) = \sqrt{k_\mathrm{p}^2 - s^2}, \quad \mathrm{Im}\,h_\mathrm{p} \geq 0, \quad k_\mathrm{p} = \frac{\omega}{c_\mathrm{p}}, \\
&h_\mathrm{s}(s) = \sqrt{k_\mathrm{s}^2 - s^2}, \quad \mathrm{Im}\,h_\mathrm{s} \geq 0, \quad k_\mathrm{s} = \frac{\omega}{c_\mathrm{s}}, \\
&R(s) = 4s^2 h_\mathrm{p} h_\mathrm{s} + (k_\mathrm{s}^2 - 2s^2)^2, \\
&T(s) = \frac{\rho_\mathrm{F} h_\mathrm{p} k_\mathrm{s}^4 - \rho h R}{\rho_\mathrm{F} h_\mathrm{p} k_\mathrm{s}^4 + \rho h R}.
\end{aligned}
$$

Above, $\boldsymbol{\varphi}_j^-(q,p,x,y,z)$ are the vector wave functions corresponding to SH (j = 1), SV (j = 2), and P (j = 3) waves. R is the Rayleigh function and T is the reflection coefficient. Note that the field in the fluid consists of an incident part $P^{(\mathrm{i})}(x,y,z)$ and a reflected part $P^{(\mathrm{r})}(x,y,z)$.

The model of the focused immersion transducer is now implemented in UTDefect by supplying the coefficients $\xi_1(q,p)$, $\xi_2(q,p)$, and $\xi_3(q,p)$. For more details, see the article by Boström and Wirdelius (1995). In order to include damping in the fluid, $\xi_1(q,p)$, $\xi_2(q,p)$, and $\xi_3(q,p)$ are multiplied by $\mathrm{e}^{-\alpha D/\cos\theta}$. As a final note, all evanescent waves are suppressed. First, only waves propagating in the negative z' direction, i.e., waves with a real and positive value on h', are considered. This approximation is reasonable since the evanescent waves only will be important a few wavelengths from the transducer. Finally, only waves that are able to reach the solid are taken into account, i.e., waves with a positive h value.

Calibration

In UTDefect, calibration may be performed on a component with a side-drilled or flat-bottomed hole. In the benchmark cases, the calibrations are performed with respect to the echo from the front surface of the component. The incidence is always normal, i.e., $\beta = 0^{\circ}$. In order to compare the experiments to UTDefect, this calibration type must be added. The signal response due to the surface of the component is computed by means of Auld's reciprocity relation (Auld, 1979). Consider the two states: (1) The component is abscent, and (2) the component is present (see Figure 3).

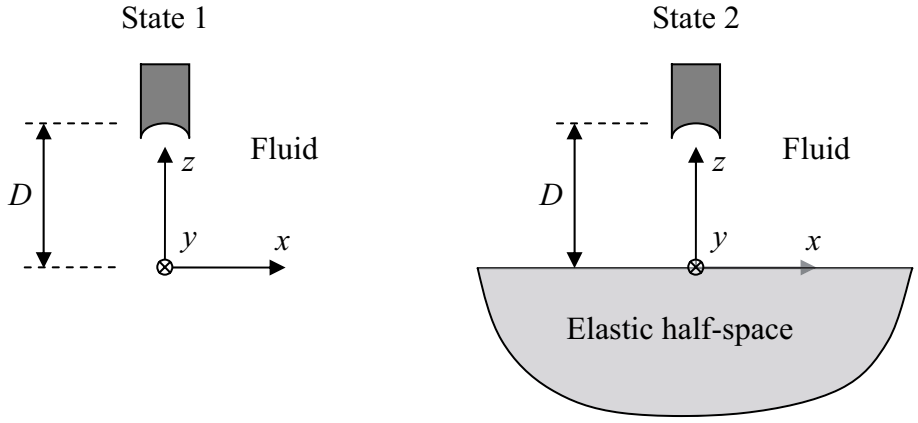

Figure 3: The two states considered in the calibration.

Auld's reciprocity relation states that the electrical transmission coefficient is given by

$$\delta\Gamma = -\frac{\mathrm{i}\omega}{4G}\int_{-\infty}^{\infty}\int_{-\infty}^{\infty}\left(U^{(\mathrm{i})}(x,y,0)P^{(\mathrm{r})}(x,y,0) - U^{(\mathrm{r})}(x,y,0)P^{(\mathrm{i})}(x,y,0)\right)\mathrm{d}x\,\mathrm{d}y, \tag{6}$$

where $U^{(\mathrm{i})}$ and $U^{(\mathrm{r})}$ are the displacement in the z direction in the fluid from the incident and reflected fields, respectively. The quantity G is (essentially) the power fed to the transducer (must be the same in both states). The displacement in the z direction is computed from the pressure as

$$U^{(\mathrm{i})} = \frac{1}{\rho_{\mathrm{F}}\omega^2}\frac{\partial P^{(\mathrm{i})}}{\partial z}, \quad U^{(\mathrm{r})} = \frac{1}{\rho_{\mathrm{F}}\omega^2}\frac{\partial P^{(\mathrm{r})}}{\partial z}. \tag{7}$$

If the fields are inserted into the reciprocity relation the resulting expression for the transmission coefficient is

$$\delta\Gamma = -\frac{\pi P_0^2}{4G\rho_{\mathrm{F}}\omega k^2}\int_0^k \frac{sT(s)\xi_0^2(s)}{h(s)}\mathrm{d}s. \tag{8}$$

The upper limit for the integration is a consequence of the omission of the evanescent waves in the fluid. The signal responses from the experiments may now be compared to the normalized response from UTDefect.

Comparison with experimental data

In this section, UTDefect is compared to experimental data from the 2004 UT Benchmark study conducted at the Center of Nondestructive Evaluation, Iowa State University, U.S.A. The benchmark study includes cases with side-drilled holes, flat-bottomed holes and a spherical cavity. In all, there are forty four cases that may be compared to experimental data. More details about the benchmark study may be found at the web page of the World Federation of NDE Centers, http://www.wfndec.org.

Immersion testing is performed in all cases and the properties of water are specified as c_F = 1.484 mm/μs, $\rho = 1000$ kg/m^3, and $\alpha = 0.2479\times10^{-4} f^2$ Np/mm, where the frequency f is given in MHz.

All experiments contain measurements from planar and spherically focused transducers. The diameter of all transducers is 12.70 mm and the center frequency is 5 MHz. The frequency spectrum used in UTDefect is given by

$$F(f) = \begin{cases} \cos^2\left(\dfrac{\pi(f - f_c)}{2\,\Delta f}\right), & -\Delta f \le f - f_c \le \Delta f, \\ 0, & \text{otherwise}, \end{cases} \tag{9}$$

with $f_c = 5\,\text{MHz}$. A 50% bandwidth is assumed, i.e., $\Delta f = 2.5\,\text{MHz}$, since this is common and not specified in the experiments. In the simulations the spherically focused transducer is divided into 20 rings, i.e., $N = 20$ (see Figure 1).

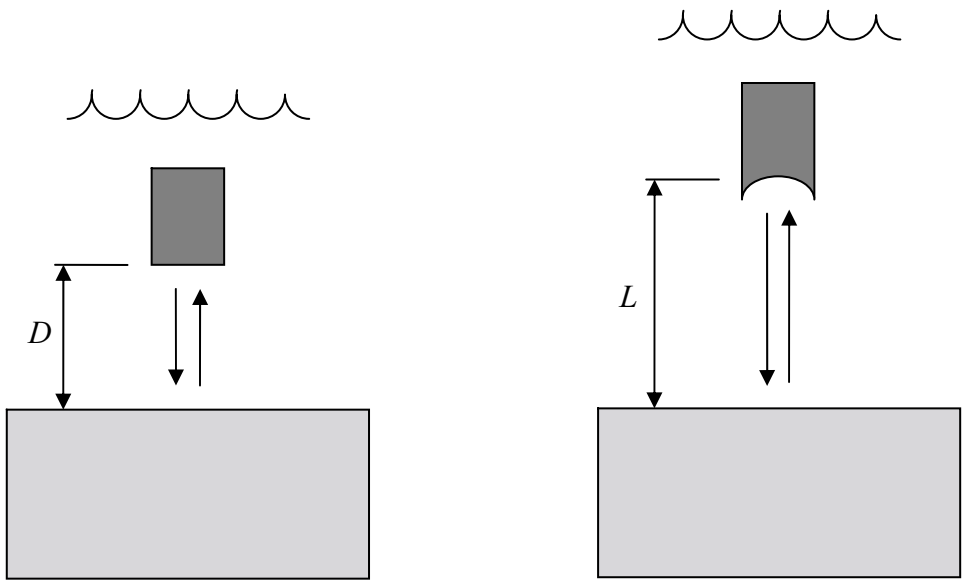

a) Calibration of the planar transducers. *b) Calibration of the focused transducers.*

Figure 4: Calibration of the experimental data.

The geometrical focal length of the spherically focused transducers is L = 172.9 mm. The experiments with the planar transducers are calibrated against the signal from the front surface of the test block at normal incidence and distance D = 50.8 mm. The calibrations when the spherically focused transducers are used are done in the same way but at a distance L = 172.9 mm, i.e., at the geometrical focal length. Figure 4 shows the calibration procedures.

Side-drilled hole

First, UTDefect is compared with the signals from two test blocks containing side-drilled holes (SDH). Block 1 contains a side-drilled hole of diameter 1 mm and block 2 contains a side-drilled hole of diameter 4 mm. In both cases, the center of the hole is located at a depth H = 25.4 mm and the material is aluminum with parameters c_p = 6.416 mm/μs, c_s = 3.163 mm/μs, and ρ = 2750 kg/m^3.

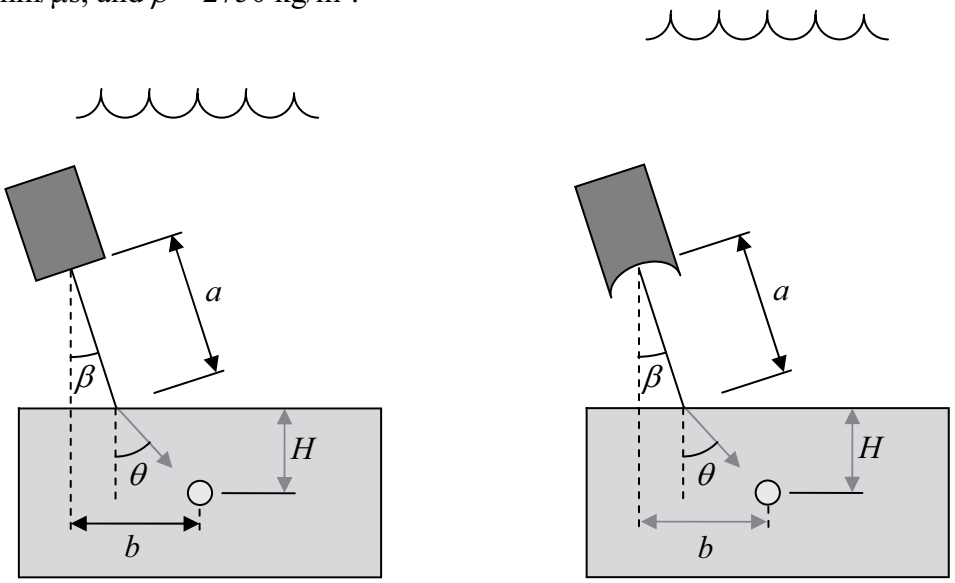

a) The setup with planar transducer. *b) The setup with focused transducer.*

Figure 5: The experimental setups in the case of the SDH.

The experimental setups are shown in Figure 5. The water path is a = 50.8 mm in all cases. The transducers are tilted in order to perform testing at oblique incidence with longitudinal (P) and shear (S) waves. The angle of the beam in the block θ is specified by the experiments. In UTDefect the input is the tilt of the transducer β, so it must be computed by means of Snell's law. In the tables, P30 means that the main beam in the block is a P wave with $\theta = 30^o$ and so on. The computed value of the angle of the transducer β is given for each case in the tables below. In the experiments, the tilt of the transducer was set to the value obtained from Snell's law. Then a line scan was performed and at the position of the strongest signal, the A-scan was recorded. In a

simulation with a tilted transducer, this is also done and the position of the strongest signal *b* is also given in the tables.

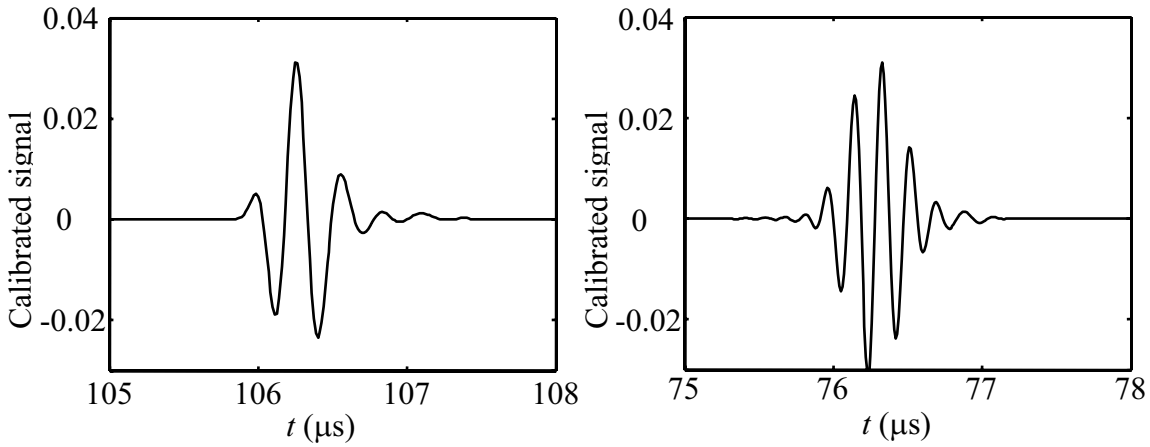

a) Experimental signal. *b) Simulated signal.*

Figure 6: Calibrated signal for the planar P0 transducer and block 1.

In Figure 6, the calibrated signals for the case of the planar transducer at normal incidence (P0) on block 1 are compared. As is seen from the figure, there are some differences. The difference in the time scale is due to gating of the experimental signal.

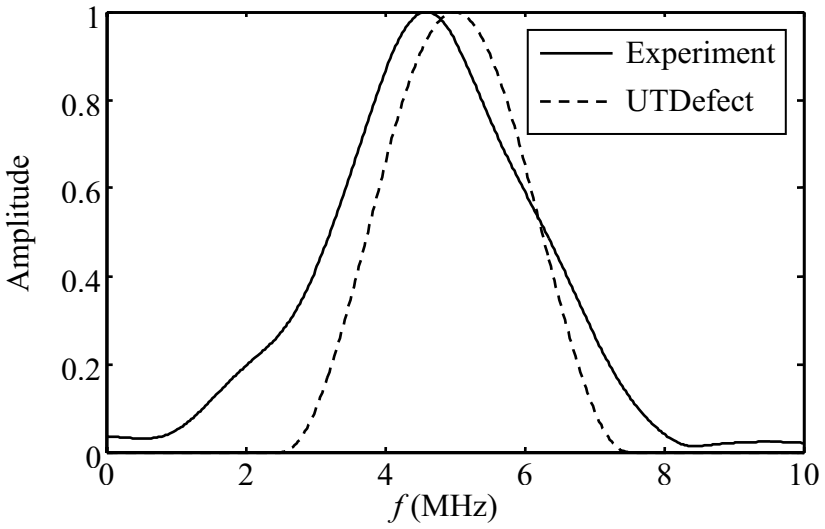

Figure 7: The true and assumed frequency spectra.

If the experimental reference signal is Fourier transformed with FFT, the spectrum shown in Figure 7 as a solid line is obtained. In Figure 7, the spectrum used in UTDefect is also shown. As may be seen from the figure, the spectra differ somewhat and this may explain the differences in the shape of the signals. The bandwidth of the experimental signal is wider resulting in a sharper pulse as is observed in Figure 6. The maximum values,

however, are in excellent agreement in this case (see Table 1 below). In some of the cases, the difference in frequency spectra may result in larger differences in the results. One way to perform more accurate simulations would be to feed UTDefect the spectrum obtained from the FFT of the reference signal directly. This has, however, not been done in this report.

First UTDefect is compared with the experimental data for the planar transducer and block 1 (the 1 mm SDH). The results of the nine cases are presented in Table 1. As is seen from the table, the cases with the P wave in the block are in excellent or good agreement with a maximum difference of 1 dB. The cases with the S wave are not in as good agreement with the experiments. Especially the case when $\theta = 60^{o}$ (S60) differs a lot from the experimental results. This behavior is consistent with the simulation results by several of the participants in the benchmark study, for example, Diligent et al. (2005), Song et al. (2005), and Schmerr Jr. et al. (2005).

Transducer	β (deg)	b (mm)	Experiment (dB)	UTDefect (dB)	Difference (dB)
P0	0	0	-30.1	-30.2	0.1
P30	6.64	26.4	-31.1	-30.6	-0.5
P45	9.41	41.7	-33.9	-32.9	-1.0
P60	11.56	62.3	-39.8	-38.9	-0.9
P70	12.55	80.1	-45.7	-45.6	-0.1
S30	13.57	38.3	-44.5	-43.2	-1.3
S45	19.38	59.3	-31.5	-29.7	-1.8
S60	23.97	84.7	-34.3	-31.5	-2.8
S75	26.95	128.5	-42.8	-41.2	-1.6

Table 1: Comparisons of results from the planar transducer on block 1.

UTDefect is then compared with the experimental data for the planar transducer and block 2 (the 4 mm SDH). The results of the nine cases are presented in Table 2. As is in the former case, the experiments with a P wave in the block are in excellent or good agreement with a maximum difference of 1.2 dB. Again, the results for the S wave are not in as good agreement with the S60 case being worst with a difference of 2.8 dB.

Transducer	β (deg)	b (mm)	Experiment (dB)	UTDefect (dB)	Difference (dB)
P0	0	0	-24.7	-24.4	-0.3
P30	6.64	26.4	-25.7	-24.8	-0.9
P45	9.41	41.7	-28.3	-27.2	-1.1
P60	11.56	62.6	-34.4	-33.1	-1.3
P70	12.55	80.4	-40.9	-39.8	-1.1
S30	13.57	38.4	-37.2	-36.0	-1.2
S45	19.38	59.4	-23.8	-22.4	-1.4
S60	23.97	84.8	-26.9	-24.1	-2.8
S75	26.95	128.3	-35.8	-34.0	-1.8

Table 2: Comparisons of results from the planar transducer on block 2.

The final comparisons with the side-drilled holes are made with the spherically focused transducer. The results are shown in Table 3 and Table 4. It is seen that the cases with the P wave are in best agreement with the experiments as for the planar transducer. With the focused transducer the agreement is in general a little bit worse than for the planar transducer. One contributing factor may be the damping model. Since the calibration for the focused transducer is performed at a much larger distance than the measurements, the effect of the damping is greater here than in the cases with the planar transducer.

Transducer	β (deg)	b (mm)	Experiment (dB)	UTDefect (dB)	Difference (dB)
P0	0	0	-24.1	-23.2	-0.9
P30	6.64	26.4	-27.5	-25.9	-1.6
P45	9.41	41.5	-32.4	-30.6	-1.8
P60	11.56	60.5	-40.3	-38.7	-1.6
P70	12.55	75.5	-46.0	-45.9	-0.1
S30	13.57	38.5	-36.9	-32.7	-4.2
S45	19.38	59.2	-27.0	-23.4	-3.6
S60	23.97	84.4	-33.4	-29.4	-4.0
S75	26.95	124.6	-43.9	-41.6	-2.3

Table 3: Comparisons of results from the focused transducer on block 1.

Transducer	β (deg)	b (mm)	Experiment (dB)	UTDefect (dB)	Difference (dB)
P0	0	0	-18.0	-17.5	-0.5
P30	6.64	26.4	-21.4	-20.1	-1.3
P45	9.41	41.7	-26.6	-24.7	-1.9
P60	11.56	60.9	-33.8	-32.8	-1.0
P70	12.55	74.2	-39.9	-40.3	0.4
S30	13.57	38.6	-28.6	-25.2	-3.4
S45	19.38	59.2	-19.4	-16.1	-3.3
S60	23.97	84.4	-26.1	-22.1	-4.0
S75	26.95	124.6	-35.7	-34.3	-1.4

Table 4: Comparisons of results from the focused transducer on block 2.

Flat-bottomed hole

Next, UTDefect is compared with the signals from three flat-bottomed holes (FBH). The holes are all located at a depth H = 25.4 mm and diameters considered are 1.191 mm (FBH #3), 1.984 mm (FBH #5), and 3.175 mm (FBH #8). The material is 1018 steel with parameters c_p = 5.94 mm/μs, c_s = 3.23 mm/μs, and ρ = 7860 kg/m^3. The experimental setups are shown in Figure 8. The water path is D = 50.8 mm in all cases and the incidence is normal.

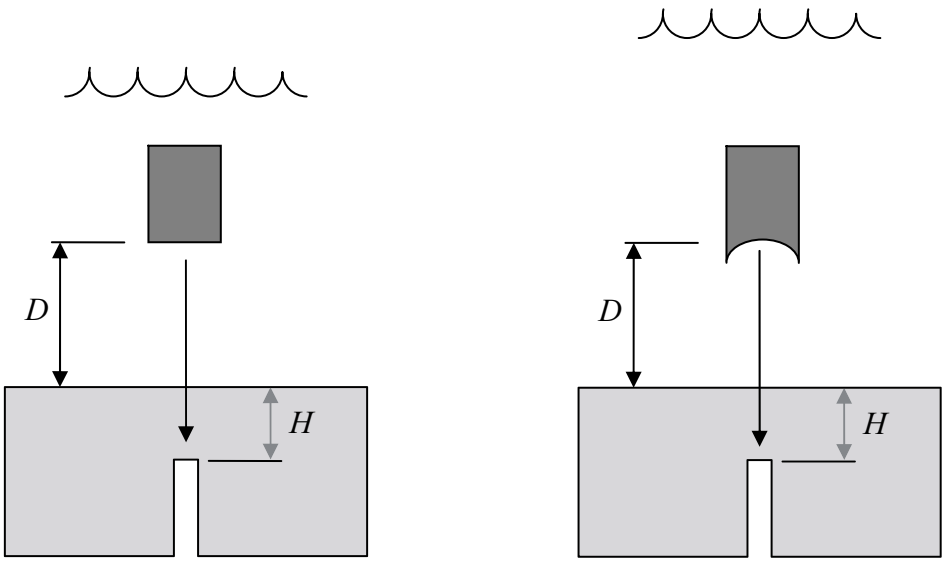

a) The setup with planar transducer. *b) The setup with focused transducer.*

Figure 8: The experimental setup in the case of the FBH.

The results of the simulations are given in Table 5 and Table 6 below. It is seen that the agreement with the experimental data is good for both transducers with a maximum difference of 1.5 dB. In the simulations, the flat-bottomed hole is taken as a circular crack. The results show that this approximation is valid for these cases.

Defect	Experiment (dB)	UTDefect (dB)	Difference (dB)
FBH #3	-47.9	-46.9	-1.0
FBH #5	-40.1	-38.6	-1.5
FBH #8	-33.2	-31.7	-1.5

Table 5: Comparisons of results from the planar transducer.

Defect	Experiment (dB)	UTDefect (dB)	Difference (dB)
FBH #3	-37.9	-37.1	-0.8
FBH #5	-30.1	-28.7	-1.4
FBH #8	-23.6	-22.1	-1.5

Table 6: Comparisons of results from the focused transducer.

Spherical cavity

Finally, UTDefect is compared to experiments performed on a spherical cavity (SPH). The cavity is located at a depth H = 19.63 mm and the diameter is 692 μm. The material is fused quartz with parameters c_p = 5.9694 mm/μs, c_s = 3.7741 mm/μs, and ρ = 2200 kg/m^3. The experimental setups are shown in Figure 9. The water path is D = 50.8 mm in all cases and the incidence is normal.

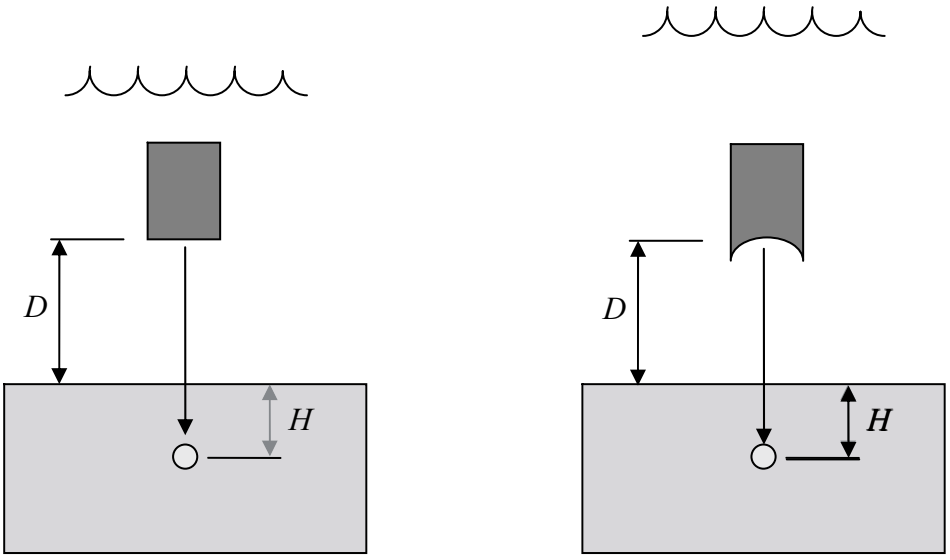

a) The setup with planar transducer. *b) The setup with focused transducer.*

Figure 9: The experimental setup in the case of the SPH.

Table 7 shows the results for the planar and spherically focused transducers. For these cases, the differences between the experiments and the simulations are as great as 5.0 dB and 3.6 dB, respectively. This is very surprising, since one would expect excellent agreement for these cases. The simulations performed by Diligent et al. (2005), Spies (2005), Song et al. (2005), and Schmerr Jr. (2005) are in much better agreement with the experiments. It is thus believed that there is an error in the implementation of the scattering by a spherical defect in UTDefect and this matter is under investigation.

Transducer	Experiment (dB)	UTDefect (dB)	Difference (dB)
Planar	-48.9	-53.9	5.0
Spherically focused	-38.1	-41.7	3.6

Table 7: Comparisons of the results.

Concluding remarks

In this paper, a simulation tool for ultrasonic nondestructive testing, UTDefect has been compared with experimental data from an international benchmark study. The experiments have been conducted with planar and spherically focused immersion transducers. The defects considered are side-drilled holes, flat-bottomed holes, and a spherical cavity. The data from the experiments are a reference signal used for calibration (the signal from the front surface of the test block at normal incidence) and the raw output from the scattering experiment. In all, forty four cases have been compared. Since UTDefect did not have any options for fluid damping and focused transducers in immersion testing, this had to be implemented. In addition, the calibration performed in the experiments (echo from the front side of the test block) was not available in UTDefect and was also implemented.

First, UTDefect was compared with data collected from experiments on two test blocks containing side-drilled holes. For each block and transducer, nine cases were compared (five P wave cases and four S wave cases). In the P cases, the difference between UTDefect and the experiments is less than 2 dB and the comparison is thus excellent or good. The difference is greater when the tilt of the transducer is increased in order to generate S waves in the block. Here, the difference is up to 4 dB which is quite large. This behavior is seen by several of the participants in the benchmark study. Also, the comparisons between the simulations and experiments are worse when the spherically focused transducer is used.

Next, UTDefect was compared with data collected from experiments on three test blocks containing flat-bottomed holes. In all cases, the incidence was normal and the agreement was found to be excellent or good (within 2 dB). Here, the differences between the simulations and experiments for the planar and focused transducers are almost identical.

In the case of the spherical cavity, the differences between the experimental data and UTDefect in the two cases are 5.0 dB and 3.6 dB, respectively. These large discrepancies are difficult to explain by means of modeling error, experimental errors and so on. It is suspected that there is an implementation error for this defect type in UTDefect and the matter needs further investigation.

References

Auld, B.A., *General Electromechanical Reciprocity Relations Applied to the Calculation of Elastic Wave Scattering*, Wave Motion, vol. 1, 1979, pp. 3-10.

Boström, A., *UTDefect – a computer program modelling ultrasonic NDT of cracks and other defects*, SKI report 95:53, Swedish Nuclear Power Inspectorate, Stockholm 1995.

Boström, A., *Ultrasonic probe radiation and crack scattering in anisotropic media*, SKI report 97:27, Swedish Nuclear Power Inspectorate, Stockholm 1997.

Boström, A., and Jansson, P.-Å., *Developments of UTDefect: rough cracks and probe arrays*, SKI report 97:28, Swedish Nuclear Power Inspectorate, Stockholm 1997.

Boström, A., *Developments of UTDefect: rough rectangular cracks, anisotropy, etc*, SKI report 00:43, Swedish Nuclear Power Inspectorate, Stockholm 2000.

Boström, A., and Wirdelius, H., *Ultrasonic probe modeling and nondestructive crack detection*, J. Acoust. Soc. Am., vol. 97, 1995, pp. 2836-2848.

Boström, A., *Ultrasonic Benchmarking with UTDefect*, Review of Quantitative Nondestructive Evaluation, Thompson, D.O. and Chimenti, D.E., eds., vol. 24, American Institute of Physics, 2005, pp. 1859-1863.

Diligent, O., Chatillon, S., Lhémery, A., and Mahaut, S., *Results of the 2004 UT Modeling Benchmark Obtained with the CIVA Software Developed at the CEA*, Review of Quantitative Nondestructive Evaluation, Thompson, D.O. and Chimenti, D.E., eds., vol. 24, American Institute of Physics, 2005, pp. 1843-1850.

Krishnamurthy, C.V., Shankar, M., and Balasubramaniam, K., *Patch Element Model for the Evaluation of Displacement Fields within an Elastic Solid from a Non-Contact Immersion Transducer: Application to the 2004 Ultrasonic Benchmark Problem*, Review of Quantitative Nondestructive Evaluation, Thompson, D.O. and Chimenti, D.E., eds., vol. 24, American Institute of Physics, 2005, pp. 1864-1871.

Lakestani, F., *Validation of mathematical models of ultrasonic inspection of steel components*, PISC III Report 16, JRC, Inst. Adv. Mat., Petten, The Netherlands, 1992.

Schmerr Jr., L.W., Kim, H.-J., Lopez, A.L., and Sedov, A., *Simulating the Experiments of the 2004 Ultrasonic Benchmark Study*, Review of Quantitative Nondestructive Evaluation, Thompson , D.O. and Chimenti, D.E., eds., vol. 24, American Institute of Physics, 2005, pp. 1880-1887.

Song, S.-J., Park, J.-S., Choi, Y.-H., Kang, S.-C., and Kim, K.-J., *Model Predictions to the 2004 Ultrasonic Benchmark Problems*, Review of Quantitative Nondestructive Evaluation, Thompson, D.O. and Chimenti, D.E., eds., vol. 24, American Institute of Physics, 2005, pp. 1872-1879.

Spies, M., *Prediction of Ultrasonic Flaw Signals and Model-to-Experiment Comparison*, Review of Quantitative Nondestructive Evaluation, Thompson, D.O. and Chimenti, D.E., eds., vol. 24, American Institute of Physics, 2005, pp. 1851-1858.

www.ski.se

STATENS KÄRNKRAFTINSPEKTION
Swedish Nuclear Power Inspectorate

POST/POSTAL ADDRESS SE-106 58 Stockholm
BESÖK/OFFICE Klarabergsviadukten 90
TELEFON/TELEPHONE +46 (0)8 698 84 00
TELEFAX +46 (0)8 661 90 86
E-POST/E-MAIL ski@ski.se
WEBBPLATS/WEB SITE www.ski.se